water

MDPI

Article

Water Temperature, pH, and Road Salt Impacts on the Fluvial Erosion of Cohesive Streambanks

Siavash Hoomehr [1], Akinrotimi I. Akinola [2], Theresa Wynn-Thompson [2,*], Waverly Garnand [3] and Matthew J. Eick [4]

1 Department of Water Resources, Dewberry Engineers Inc., New York, NY 10001, USA; shoomehr@dewberry.com
2 Department of Biological Systems Engineering, Virginia Tech, Blacksburg, VA 24061, USA; akinola@vt.edu
3 Stantec Consulting Services Inc., Santa Barbara, CA 93101, USA; Waverly.Garnand@stantec.com
4 Department of Crop and Soil Environmental Sciences, Virginia Tech, Blacksburg, VA 24061, USA; eick@vt.edu
* Correspondence: tthompson@vt.edu; Tel.: +1-540-231-2454

Received: 24 January 2018; Accepted: 8 March 2018; Published: 10 March 2018

Abstract: Increasing human populations and global climate change will severely stress our water resources. One potential unforeseen consequence of these stressors is accelerated stream channel erosion due to increased stream temperatures and changes in stream chemistry, which affect the surface potential and hence the stability of soil colloids. The objectives of this study were to determine the effect of water temperature, pH, and salinity on streambank erosion rates; determine how erosion rates vary with clay mineralogy; and, explore the relationship between zeta potential and erosion rate. Remolded samples of natural montmorillonite- and vermiculite-dominated soils were eroded in a recirculating hydraulic flume under multiple shear stresses (0.1–20 Pa) with different combinations of water temperature (10, 20, and 30 °C), pH (6 and 8), and deicing salt (0 and 5000 mg/L). The results show that erosion rates significantly increased with increasing water temperature: a 10 °C increase in water temperature increased median erosion rates by as much as a factor of eight. Significant interactions between water pH and salinity also affected erosion rates. In freshwater, erosion rates were inversely related to pH; however, at high salt concentrations, the influence of pH on erosion rates was reduced. Results of this study clearly indicate water chemistry plays a critical role in the fluvial erosion of cohesive streambanks and suggest that channel protection efforts should include controls for stream temperature, in addition to peak flow rates, to maintain channel stability.

Keywords: fluvial erosion; cohesive soil; streambank retreat; water temperature; stream pH; salinity

1. Introduction

Streambank retreat and the resulting sediment pollution threaten the sustainability of urban stream systems and surface water supplies. Urbanization increases stormwater runoff quantity, timing, and chemistry: the resulting channel enlargement and migration damage the adjacent urban infrastructure, including sewer and water lines, utilities, buildings, and bridges [1]. Once entrained, the eroded sediment becomes a water pollutant. Excess suspended sediments reduce the diversity and abundance of aquatic organisms, increase the need for dredging, reduce hydropower and water supply reservoir capacity, increase drinking water treatment costs, and serve as a carrier for contaminants such as phosphorus, bacteria, heavy metals, pharmaceuticals, and pesticides. In the United States alone, the annual cost of water erosion due to on-site and off-site damages, including nutrient loss, habitat depletion, sedimentation, and flooding, as well as the cost associated with erosion prevention, have been estimated as greater than 20 billion dollars [2].

Streambank retreat typically occurs by a combination of two main processes: fluvial erosion and bank failure (Figure 1a). Fluvial erosion is the direct removal of soil particles or aggregates from the channel boundary by stream flow [3], while the collapse of streambanks due to the mechanical instability of the bank is referred to as "bank failure" or "mass wasting" [4]. Fluvial erosion and bank failure work in concert to cause channel enlargement and/or migration. While bank failure is a dramatic event, preventing excessive fluvial erosion is key to preventing streambank instability [5]. Unfortunately, there is a relative lack of information on fluvial erosion as opposed to mass wasting [6,7].

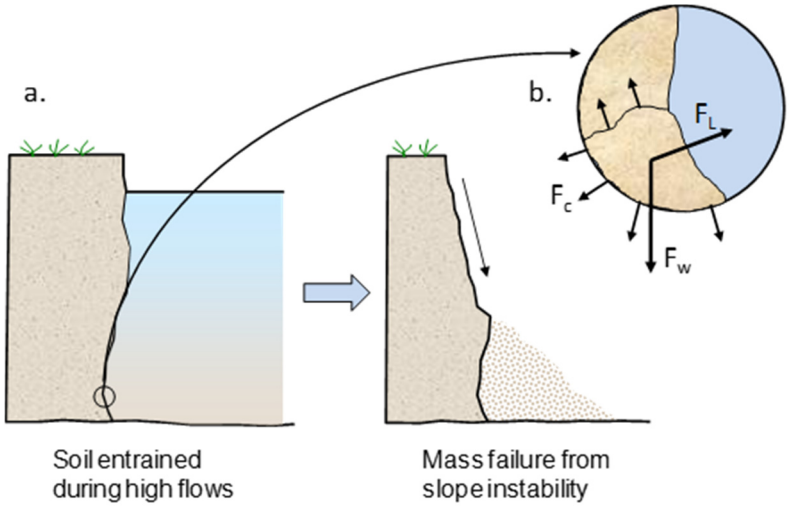

Figure 1. (**a**) Cyclical process of streambank retreat and (**b**) force balance on a soil aggregate, where F_w is the submerged body force, F_L is the hydraulic lift force, and F_c is the cohesive force holding the aggregate to the streambank. For visual clarity, the drag force is not shown.

Fluvial erosion can be modeled as a balance between applied hydraulic forces (F_L) and resisting soil forces (Figure 1b). Noncohesive soils (particle size >50 μm) are held onto the streambank or stream bed primarily by particle weight (F_w). Unlike noncohesive soils, cohesive soils are bound together via multiple mechanisms related to interlayer clay bonding, sesquioxide-cement bonds, and organic secretions from roots and soil microorganisms (F_c) [8,9]. The streambanks of many single thread channels consist of cohesive soils formed by the deposition of suspended sediment on the floodplain [10,11]. While multiple studies have investigated the fundamental processes and drivers of streambank erosion, the complexity of cohesive soil responses to changing flow chemistry has complicated the development of predictive models of cohesive erosion that can be used to forecast streambank erosion arising from changing environmental conditions [12].

While cohesive soils are a mixture of sand, silt, and clay, because of their small size (<2 μm), high charge density, and large surface area, the clay fraction strongly influences soil cohesive behavior [13]. Clay minerals are layer silicates and metal oxides bound primarily by van der Waals interactions [14]. The surface charge of clay minerals may be constant due to isomorphic substitutions in the mineral structure or variable (i.e., pH-dependent) due to ion adsorption/desorption of surface functional groups [15,16]. These different surface charges strongly influence the behavior and response of cohesive soils to water [17,18].

Since clays must remain electrically neutral, an equal charge of opposite sign must surround the charged particle. Furthermore, to satisfy the system's electroneutrality requirement, the surface charge is satisfied by positive adsorption of counterions and negative adsorption or (exclusion) of co-ions. The charged surface, including the counter- and co-ions, is referred to as the electric double layer (EDL) and, in natural systems, the size of the EDL influences the stability of the clay [18]. For example, a large EDL results in colloidal instability (i.e., repulsion) while a small or compressed EDL results in colloidal stability (i.e., attraction.). In aqueous soil systems, the EDL thickness depends on the concentration

of ions in pore water and the charge and size of the hydrated radii of the counterion [18]. Electrical double layer thickness is inversely proportional to counterion charge and ionic strength and directly proportional to counterion size [19]. As a result, cohesive soil erosion is related to characteristics of both the soil and the eroding fluid [9,20].

During storm events, streambank soils react nearly instantaneously to changes in stream water pH, temperature, and salt concentration, influencing the size of the EDL and the stability of soil colloids [17,21]. With increasing human populations and global climate change, streambank erosion could potentially occur in currently stable stream systems and accelerate in existing unstable systems. For example, summer thunderstorms in urban watersheds can increase stream temperature >7 °C [22]. During winter storm events, high concentrations of sodium in deicing salts can increase the size of the EDL; stream chloride concentrations of 11,200 mg/L (ocean water is ~19,000 mg/L) due to road deicing salts have been measured in winter [23]. The impact of global climate change on average stream temperature is already evident in some stream systems with increases in mean annual stream temperatures of 2–5 °C predicted for the contiguous US [24]. The impact of these changes on stream stability has yet to be fully quantified; however, research by Wynn and Mostaghimi [5] indicates a 2 °C rise in stream temperature alone could increase erosion rates by 30%. These potential changes in erosion occurrence and rate need to be quantified in order to identify the areas that are at risk for increased stream channel erosion and to develop mitigation strategies as cohesive soils are ubiquitous in the majority of river systems [9,25].

The overall goal of this project was to evaluate the impact of changes in stream chemistry—commonly observed in urban watersheds and expected to occur due to climate change—on streambank fluvial erosion. Specifically, changes in cohesive streambank soil erosion rates with changes in stream pH, temperature, and salt concentration were measured to assess the possible impacts of land use and climate change on stream stability. Study results indicate that erosion rates increase significantly with increasing stream temperatures, regardless of soil type. Interactions between water pH and salt concentrations also influence cohesive streambank erosion rates, with increases in erosion rate observed with decreases in stream pH, but only for water of low ionic strength.

2. Materials and Methods

The effects of changes in water temperature, pH, and deicing salt on the erosion of cohesive soils were investigated by subjecting remolded soil cores to a series of shear stresses and measuring the soil erosion rate. The process was repeated for combinations of average water temperature (10, 20, and 30 °C), pH (6 and 8), and NaCl deicing salt (0 and 5000 mg/L), hereafter referred to as "environmental conditions" that are observed in natural systems. Erosion rate for each environmental condition was measured by tracking the amount of advancement necessary to keep the sample flush with the wall for the duration of the experiment. Parametric and non-parametric statistical analyses were used to determine significant differences in average erosion rates for the samples under different environmental conditions.

The erosion experiments were conducted using an 8 m × 1 m × 0.4 m recirculating flume (Engineering Laboratory Design Inc., Lake City, MN, USA). An artificial wall was built within the channel to allow the soil cores to be placed vertically within the wall, an orientation similar to an eroding streambank. This position allowed erosion to occur either as fluvial erosion or as mass wasting. In prior research with samples placed in the flume bed, both detachment and transport were necessary to move the soil particles [26–29]. By placing the sample in a vertical position, the mode of soil loss–fluvial erosion or mass wasting—could be distinguished. This setup also narrowed the flume width to 40 cm and reduced the volume of water needed to run the flume from 5000 L to 3700 L. The wall was created from 1.25-cm thick PVC sheeting with a wooden structure for support. At the flume entrance, thin Plexiglas was used to create a curved wall to gently transition the width of the channel from 1 m at the flow straightener to 0.4 m.

To determine the best location for the soil core placement, velocity profiles, under multiple flow conditions, were measured down the center of the test section and normal to the wall at varying depths with a Vectrino II Acoustic Doppler Profiler (ADP) velocimeter (Nortek AS, Bærum, Norway). The ADP measures velocities in three dimensions over a 2-cm range located 4 cm from the probe head; measurements were taken in 1-mm intervals, or bins, throughout the sampling range at a rate of 50 Hz. The probe head was placed in a horizontal position (Figure 2) to collect a centerline velocity profile perpendicular to the wall. The four flume settings used in this study are provided in Table 1. The applied shear stress for each test was determined using the law of the wall.

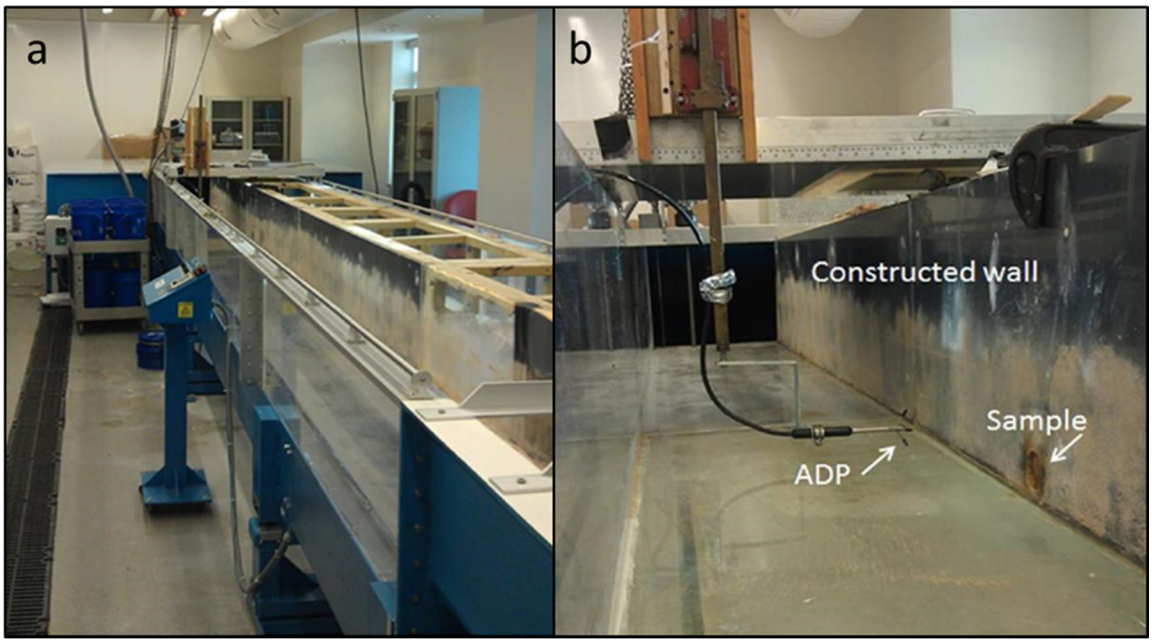

Figure 2. (**a**) Flume channel and (**b**) close-up of sample location.

Table 1. Flume settings used for each test condition.

Setting	Tailgate Height (cm)	Channel Slope (%)	Flow Depth (cm)	Flow Rate (m^3/s)	Target Wall Shear Stress * (Pa)
1	10	0.5	14	0.017	0.2
2	5	0.5	9	0.017	0.5
3	0	0.5	9	0.036	3.0
4	0	1.0	8	0.055	6.5

* As determined at the center of the sample.

The sample placement point, 5.24 m from the channel inlet, was chosen where the flow was fully developed but secondary flows and tailwater effects were minimized. The center of the sample was located 4.5 cm from the flume bed (Figure 2), which was low enough to completely submerge the sample at the lowest flow depth and still accommodate the depth needed for the ADP probe. The sample support bracket within the vertical wall was designed so the core could be advanced from behind the vertical wall in 1-mm increments. Soil advancements kept the sample flush with the wall after erosion events to minimize the development of local turbulent structures on the surface of the soil core. To compensate for the roughness of the sample surface and to allow full development of the wall boundary layer, sand was adhered to the constructed wall surface with spray adhesive. The sand utilized (Premium Play Sand No. 1113, Quikrete, Atlanta, GA, USA) had a D_{50} of 0.15 mm and a D_{84} of 0.3 mm.

Two natural soils with different clay mineralogies were chosen to represent different clay properties. The vermiculite-dominated Ross soil (Cumulic Hapludolls, fine-loamy, mixed, mesic) was acquired from the top 10–40 cm of the lowest river terrace located next to the New River at Whitethorne, VA. This soil was previously characterized as 20.4% clay, 40.2% sand, and 39.4% silt. The clay fraction of the vermiculite soil was comprised of 35% hydroxyl interlayered vermiculite, 10% vermiculite, 10% mica, 15% kaolinite, 13% quartz, 10% chlorite, and 6% smectite [30]. The montmorillonite-dominated McGary soil (fine, mixed, active, mesic Aeric Epiaqualfs) was obtained along the banks of Stroubles Creek in Blacksburg, Virginia. This soil was composed of 47% sand, 42% silt, and 11% clay, with the clay fraction comprising of 60% montmorillonite/kaolinite, 35% illite/hydroxyl interlayered vermiculite, 3% chlorite, and 2% quartz [31].

Although these two natural soils contained multiple different clay minerals, they have been designated in this paper as "vermiculite dominated" and "montmorillonite dominated" soils to reflect the most active clay type in the soil and for convenience. Vermiculite is a 2:1 layer clay mineral classified as semi-expanding due to its restricted potential to expand when exposed to water. Montmorillonite is also a 2:1 layer clay mineral but unlike vermiculite is fully expanding as a result of low electrostatic attraction between the clay sheets, which allows a relatively easier adsorption of water between the clay sheets.

The soils were air-dried, pulverized using a mortar and pestle to remove the macrostructure, and passed through a 2-mm mesh. For each soil, multiple combinations of bulk densities were tested to determine a density that would erode under the highest flume shear stress setting, but also had sufficient soil strength and cohesion to maintain soil structure while saturated.

To construct each soil core, the moisture content of the air-dried mass of soil was determined and the amount of deionized water necessary to bring the soil to a pre-determined moisture content was added. The soil was then thoroughly stirred until a uniform consistency was achieved and poured into a 5 cm by 5 cm aluminum ring in a series of three soil layers. Each soil layer was compacted with a 4.64-kg slide hammer by raising the hammer to a height of 50 cm and allowing it to fall freely. The number of hammer blows required to achieve the predetermined bulk densities for each soil is listed in Table 2. Each layer of compacted soil was scarified before compacting the next layer.

Table 2. Specifications for soil core creation.

Clay Type	Bulk Density (g/cm^3)	Clay (%)	Soil Moisture Content at Compaction (%)	Hammer Blows Per Layer
Vermiculite	1.5	20.4	7.5	4
Montmorillonite	1.3	11.0	4.7	3

Once created, the soil cores were soaked overnight in deionized water with a mesh fabric placed over both ends of the core to maintain the soil structure while allowing water to permeate the core. The saturated cores were then placed on a pressure plate (5 bar pressure plate extractor cat. #1600, Soilmoisture Equipment Co., Santa Barbara, CA, USA) at a vacuum pressure of 1/3 bars or 4.3 psi for a period of three days to bring the samples to field capacity. Once removed from the pressure plates, samples were stored in a sealed glass jar over a layer of water to maintain the sample moisture content. Samples were tested the same day they were removed from the pressure plates.

Testing began by setting the flume to the lowest shear stress setting. Next, the soil core was placed in the soil advancer system within the flume wall and advanced until the sample protruded approximately 3 mm from the wall. The protruding sample was shaved flush with the wall using a wire. The sample was then covered with a plastic tray and the flume turned on. Covering the surface of the soil prevented shear stress on the soil surface while flow developed within the flume channel. Once uniform flow was achieved (50–130 s), the sample was uncovered and the distance from the probe head to the sample surface was monitored at a rate of 50 Hz. Erosion was assumed to have occurred when the boundary distance reading increased 1 mm. Preliminary testing of the ADP

determined that the distance to boundary reading varied by an average of 0.01 to 0.27 mm, with a maximum deviation of 0.64 mm [32]. Therefore, changes in the distance to the boundary of 1 mm were considered indicative of soil erosion. Following each 1 mm of erosion, the soil sample was advanced to maintain the soil surface flush with the flume wall. The initial and final positions of the sample advancer were recorded as the total eroded depth for each experiment to provide a secondary measure of erosion. Each soil core was eroded for 15 min. This duration was chosen such that the total amount of soil eroded during the run did not exceed the length of the soil core. After each 15-min flume run, the sample was again advanced and shaved flush with the wall to prepare a fresh surface for the next higher shear stress (Table 1). Three soil cores (replicates) were created and tested for each soil type and environmental condition. This process was repeated for all four pre-determined flume settings (Table 1), or until all three cores were used. Each combination of soil type and environmental condition was replicated three times at each of the four shear stress settings.

The target water temperatures, pHs, and salt concentrations were 10, 20, and 30 °C, 6 and 8, and 0 and 5000 mg/L, respectively. Tap water from the New River Valley Water Authority was used in the flume (20 °C, pH = 8, and salt = 0 mg/L). Two 1000-W aquarium heaters (True Temp T-1000, Transworld Aquatic Ent., Inglewood, CA, USA) were installed in the flume tank to increase the water temperature to 30 °C, while 19-liter plastic buckets with ice were placed in the flume tank to reduce the water temperature to 10 °C without changing the water chemistry. The water pH was adjusted using technical grade 0.01 M HCl and KOH. Sodium chloride deicing rock salt (Scotwood Industries, Inc., CAS #007647-14-5, Overland Park, KS, USA) was added at a concentration of 5000 mg/L to increase the ionic strength of the water. Water temperature was measured continuously by the ADP; water pH and conductivity were tested at the start and end of each erosion experiment using an Oakton pH/CON 10 meter (Vernon Hills, IL, USA). Because the flume pump continuously heated the water (as a byproduct of pump operation), actual water temperature ranges were 9.1–12.2, 19.4–21.2, and 29.2–30 °C, while pH ranged over 5.9–6.1 and 7.9–8.1.

Since colloidal science research indicates that the majority of activity at the soil interface is strongly related to the electrochemical forces present at this layer [33], a measure of the electrical interactions of ions at the soil–water interface for all environmental conditions was investigated. The double layer model is used to visualize the ionic environment adjacent to a charged colloid. According to the double layer theory, the charges on the surface of clay minerals, assumed to be point charges in an ionic solution, are balanced by oppositely charged ions firmly attached to the surface of the colloid, which is known as the Stern Layer. Additional counterions are still attracted to the colloid and this dynamic equilibrium results in the formation of a diffuse layer of counterions. In a similar but opposite way, there is a lack of co-ions adjacent to the surface. The attached counterions in the Stern Layer and the unequal distribution of counter- and co-ions in the diffuse layer are referred to as the electrical double layer. The double layer forms due to the concept of electroneutrality that in turn causes an electrokinetic potential (zeta potential) between the surface of the colloid and the aqueous environment. Since the thickness of the double layer is inversely related to the electrolyte concentration [34], it is reasonable to assume that cohesive soil erosion, which is a surface process, is related to the electrokinetic potential, or zeta potential. Zeta potential is a measure of the stability of the colloidal interface and becomes more electronegative with increasing electrolyte concentration due to the compression of the double layer [35]. To explore the relationship between zeta potential and erosion rate, zeta potentials at each environmental condition were measured using a Zetasizer 3000HS (Malvern Instruments, Worcestershire, UK). Based on preliminary data and particle size, the voltage applied to the capillary cell was set at 100 V and a Henry function (f(Ka)) of 1.5 was used to calculate the zeta potential.

Following flume testing, the erosion rate and shear velocity for each erosion experiment was calculated using the ADP data. For all test runs, the first millimeter of erosion was disregarded since this layer was disturbed while preparing the cores; the erosion rate was calculated by dividing the total advancement after the first millimeter of erosion by the time between the instance of the first

millimeter of erosion and the end of the 15-min run. Any event where the core eroded more than 2 mm within 5 s was classified as a mass wasting episode and was not included in the erosion rate calculations. Velocity profile data from the ADP were used to determine the shear velocity (a measure of shear stress) for each run using the rough equation for the law of the wall given in Equation (1) [36]:

$$\mathrm{u}(y) = \frac{\mathrm{u}^*}{\mathrm{k}} \ln\left(\frac{y}{y_0}\right), \quad (1)$$

where u(y) is the time-averaged streamwise velocity at a distance y from the wall (m/s); u* is the shear velocity (m/s); k is Von Karman's constant (0.4); y = distance from the wall (m); and y_0 = distance at which the velocity is zero (m).

To determine u(y) for each run, the velocity time series was filtered by removing data points with correlations less than 40% and with signal-to-noise ratio (SNR) values less than 10 dB. Overall, if more than 15% of the time series for a particular u(y) were filtered out, the entire 1-mm bin was removed. Following post-processing, u(y) were averaged for the entire 15-min run. The value of u* was then determined by fitting a line with a zero intercept to the regression of u(y) against ln(y/y_0). Because y_0 values change with flow conditions and changes in the soil surface, each y_0 value was adjusted until the best data fit was obtained. In any of the profiles, data points that fell outside the logarithmic profile, in either the buffer layer or the outer layer, were not used in the calculation. Also, flume runs in which the velocity profiles had four or fewer points remaining after signal processing were removed from the overall study data. Shear stress was calculated using the following equation:

$$\tau_0 = \rho \mathrm{u}^{*2}, \quad (2)$$

where τ_0 is the shear stress (Pa); ρ is the water density at each temperature (kg/m^3); and, u* is the shear velocity (m/s). To account for differences in the applied shear stresses between runs, the erosion rate for each test run was divided by the corresponding shear velocity to obtain dimensionless erosion rates (Er/u*) on which statistical analyses were performed.

To investigate the effect of water temperature, pH, and salt on the erosion of clay-dominated natural soils, Er/u* values were analyzed using the JMP statistical software package (Version 13.0, Cary, NC, USA). The data, separated by soil type, were analyzed using parametric ANOVA, Student's t and Tukey–Kramer honest significant difference (HSD) tests, as well as non-parametric pairwise Wilcoxon rank-sum tests. Since the dimensionless erosion data for each soil type were not normally distributed according to the Shapiro–Wilk test [37], the normality of the data was first improved using Box-Cox transformations [38] prior to the parametric tests. To ensure that all null dimensionless erosion data were preserved during the Box-Cox transform, the erosion data were first adjusted as follows:

$$J(y) = \frac{y + yy}{yy}, \quad (3)$$

where yy is the lowest non-zero dimensionless erosion rate. This procedure essentially moved the zero values to unity before applying a Box-Cox transformation defined as follows:

$$T(J(y)) = \frac{J(y)^{\lambda} - 1}{\lambda}, \quad (4)$$

where y is the dimensionless erosion data, $T(J(y))$ is the transformed dimensionless erosion data, and λ is the Box-Cox parameter. The λ that resulted in the most normal data, measured by the Anderson–Darling test [39], was -0.3 for the vermiculite-dominated soil data and 0.2 for the montmorillonite-dominated soil data. While the transformation improved the normality of the data, the Shapiro–Wilk and the Anderson–Darling tests indicated the data still did not follow a normal distribution. Following the normalization procedure, full factorial parametric regressions were performed on the transformed data by soil type to evaluate the main and interaction effects on the

erosion rates. Post hoc tests to compare between levels of the significant factors were performed using pairwise Student's *t*-tests when the number of levels in the factor was two or Tukey–Kramer HSD tests when the factor level was more than two.

3. Results

Erosion rates were calculated as the sum of the change in the distance-to-boundary reading by the ADP and confirmed by manual measurements. Each test condition and shear stress combination was repeated three times. Erosion rates of individual tests ranged from 0 mm in 15 min to 41 mm in 15 min (Table S1). To minimize the sample and test variability, three cores were prepared for each environmental condition and testing for a given environmental condition was halted when all three cores had been eroded. As a result, environmental conditions that resulted in high erosion rates were not repeated at higher shear stresses. To account for variability in erosion rates caused by slight differences in the applied shear stress and to create dimensionless erosion rates, the erosion rate (Er) for each test was divided by the shear velocity (u*) for that test.

Figure 3 shows the computed dimensionless erosion rates (Er/u*) over the range of flow temperatures, pHs, and salt concentrations tested. Although there was variability in the erosion rates, distinct trends were apparent. An increase in erosion rate with water temperature was observed, irrespective of pH and salt concentration. Median erosion rates at 30 °C for the montmorillonite and vermiculite soils were 2.1 and 1.6 times higher, respectively, than at 20 °C, across all combinations of water pH and salt concentration. For freshwater at pH 6, the median Er/u* at 20 °C was eight times higher than the median Er/u* at 10 °C for both soils. There was also a clear indication of interaction between pH and salt concentration. For example, for freshwater and all soil types and flow temperatures, increasing water pH from 6 to 8 resulted in a reduction in Er/u*. In contrast, at a salt concentration of 5000 mg/L, changes in Er/u* with increases in either water temperature or water pH were less significant, except for the montmorillonite-dominated soil at the highest flow temperature.

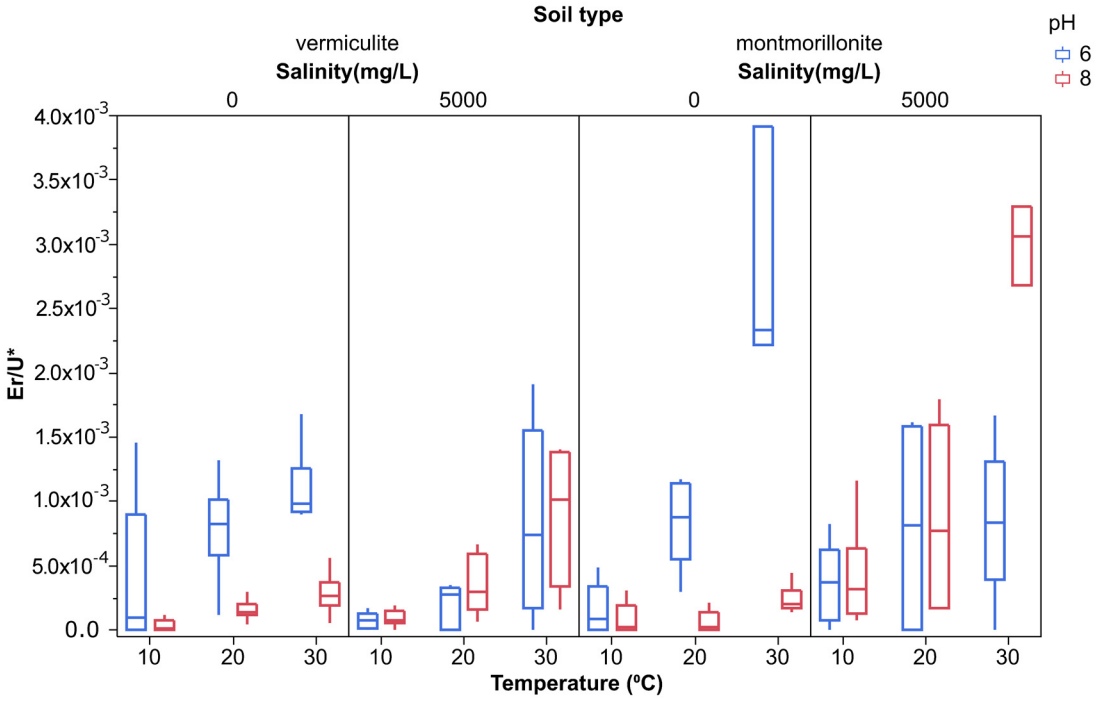

Figure 3. Effect of changing temperature, pH, and rock salt concentration on dimensionless erosion rates (Er/u*) for natural soils dominated by vermiculite and montmorillonite clay minerals. The box shows the interquartile range with the median. The vertical lines indicate the range of the data.

To investigate the statistical significance of the changes in the mean dimensionless erosion rate with changing environmental conditions, a full factorial regression was performed for both soils. Test results are provided in Table 3 (montmorillonite soil) and Table 4 (vermiculite soil). These results clearly show that Er/u* significantly increased with increasing water temperature ($p < 0.0001$) for both soils.

Table 3. Results of full factorial regression investigating the effect of changing temperature, pH, and rock salt concentration on mean dimensionless erosion rates (Er/u*) for a natural soil dominated by montmorillonite clay minerals ($r^2 = 0.57$, alpha = 0.05).

Source	Sum of Squares	F Ratio	*p*-Value
Temp	192.32635	23.7273	**<0.0001**
pH	13.01231	3.2107	0.0770
Temp*pH	9.10454	1.1232	0.3304
Salinity	40.60450	10.0187	**0.0022**
Temp*Salinity	6.91366	0.8529	0.4301
pH*Salinity	146.92810	36.2530	**<0.0001**
Temp*pH*Salinity	61.82427	7.6273	**0.0009**

Table 4. Results of full factorial regression investigating the effect of changing temperature, pH, and rock salt concentration on mean dimensionless erosion rates (Er/u*) for a natural soil dominated by vermiculite clay minerals ($r^2 = 0.45$, alpha = 0.05).

Source	Sum of Squares	F Ratio	*p*-Value
Temp	18.29565	29.4277	**<0.0001**
pH	0.58175	1.8714	0.1745
Temp*pH	0.11406	0.1835	0.8327
Salinity	0.12476	0.4013	0.5279
Temp*Salinity	0.68730	1.1055	0.3352
pH*Salinity	5.31600	17.1011	**<0.0001**
Temp*pH*Salinity	0.27657	0.4448	0.6422

The interaction of stream pH and salt concentration was also highly significant for both soils ($p < 0.0001$). Furthermore, for the montmorillonite-dominated soil, the concentration of deicing salt ($p = 0.0022$) and the interaction of water temperature, pH, and salt concentration ($p = 0.0009$) significantly influenced soil erosion rates. Although changes in erosion rate with water pH were not statistically significant, the *p*-values were low ($p = 0.0770$ for montmorillonite and $p = 0.1745$ for vermiculite), suggesting that water pH alone may influence cohesive soil erosion rates.

Because the data did not follow a normal distribution, even after transformation, two additional tests were conducted to support the findings of the full factorial regression. Because the non-normality of data used for the initial analyses was largely a result of a number of zero erosion data points, these values were removed from the transformed data and the parametric analyses were repeated. Results of the full factorial regression without zero values confirmed the initial results (Tables 3 and 4) and provided additional support that pH was a significant factor in the erosion rate of both the montmorillonite soil ($p = 0.0002$) and the vermiculite soil ($p < 0.0001$).

To further explore the changes in dimensionless erosion rates with changes in water chemistry, post hoc tests were performed on the means using pairwise Student's *t*-test when the number of levels in the factor was two (vermiculite) and Tukey–Kramer honest significant difference (HSD) test when the factor level was more than two (montmorillonite). Additionally, since normality tests indicated the data for both soil types were not normally distributed, separate pairwise non-parametric comparisons of median Er/u* were performed using the Wilcoxon rank-sum test (also known as the Mann–Whitney U test) at all combinations of temperature, pH, and salinity levels. While these

non-parametric tests have less power than a full factorial regression, they do not assume the data follow a Gaussian distribution and are useful for small sample sizes.

For the vermiculite, the results of the Wilcoxon test (Table 5) generally support the findings of the full factorial regression, which shows that the dimensionless erosion rate increased with increasing temperature. The Wilcoxon results indicate that increases in median Er/u* were significant at all temperatures and salinities when the pH was 8 (alpha = 0.05). At pH 6, the increase in median Er/u* was only significant between water temperatures of 10 °C and 30 °C. The Student's *t*-test indicates that differences in mean Er/u* were also statistically significant for all combinations of pH and salinity (not included in Table 5, since only two factors were tested). Overall, the Wilcoxon test reveals that differences in the median erosion rate of the vermiculite-dominated soil due to pH were only significant at the lower salinities, suggesting the higher salt concentrations may negate the influence of water pH on soil charge. The pairwise comparisons for differences due to salt concentration alone were significant in only three of the six comparisons (Table 5), supporting the finding of the Student's *t*-test that the combined influence of pH and salinity is an important factor in the fluvial erosion of the vermiculite-dominated soil.

Results of the Wilcoxon tests and the Tukey–Kramer HSD test for the montmorillonite soil are also shown in Table 5. As with the vermiculite soil, increases in the montmorillonite soil erosion rates with increasing water temperature at pH 6 were statistically significant for the low salinity water but not for the higher salinity water. At pH 8, the influence of water temperature was less clear, as the tests of the mean and median dimensionless erosion rates gave conflicting results, except for comparisons of the high erosion rates measured at 30 °C. Similarly, Er/u* decreased with increasing pH of the fresh water at 20 °C and 30°C, but the only significant difference due to pH for the salt water was observed at 30 °C. Changes in the erosion rates due to increased salinity were more significant at pH 8. Overall, results of the pairwise non-parametric Wilcoxon test support the results of the parametric Tukey–Kramer HSD test, which indicate there were significant interactions between water temperature, pH, and salinity for the montmorillonite-dominated soil.

To test the hypothesis that the soil erosion rate is related to the soil surface electrical potential and that the soil surface potential changes with changing water chemistry, the zeta potential for each soil was measured under the environmental conditions used for the erosion testing. However, regression analysis showed that zeta potential was only weakly correlated to the logarithmic transform of Er/u* for the montmorillonite-dominated soil (r^2 = 0.19) and the vermiculite-dominated soil (r^2 = 0.13). This weak correlation is likely due to the small amount of pH-dependent charge that developed in the dominant clays, as compared to permanent charge, and indicates that the zeta potential would not be a strong predictor of the susceptibility of cohesive soils to fluvial erosion.

Table 5. Comparisons of the dimensionless erosion rates. The capital letters indicate results of the pairwise non-parametric Wilcoxon test of the medians and lowercase letters indicate the results of the parametric Tukey–Kramer HSD comparison of the means for the montmorillonite soil. Wilcoxon results for the vermiculite-dominated soil are in the lower left corner and are italicized and bolded. Yellow, blue, and orange cells indicate salinity, pH, and temperature comparisons, respectively.

	T10P6S1 [1]	**T10P6S2**	**T20P6S1**	**T20P6S2**	**T30P6S1**	**T30P6S2**	**T10P8S1**	**T10P8S2**	**T20P8S1**	**T20P8S2**	**T30P8S1**	**T30P8S2**
T10P6S1	---	N,n	D,d	N,n	D,d	D,d	N,n	N,d	N,n	D,d	N,n	D,d
T10P6S2	***N*** [2]	---	D,n	N,n	D,d	N,n	D,d	N,n	D,n	N,d	N,n	D,d
T20P6S1	***N***	***D***	---	N,n	D,d	N,n	D,d	N,n	D,d	N,d	D,n	D,d
T20P6S2	***N***	***N***	***D***	---	D,d	N,n	N,n	N,n	N,d	N,d	N,n	D,d
T30P6S1	***D***	***D***	***N***	***D***	---	D,d	D,d	D,d	D,d	D,n	D,d	N,d
T30P6S2	***N***	***D***	***N***	***N***	***N***	---	D,d	N,n	D,d	N,n	D,d	D,d
T10P8S1	***N***	***N***	***D***	***N***	***D***	***D***	---	D,n	N,n	D,d	D,n	D,d
T10P8S2	***N***	***N***	***D***	***N***	***D***	***D***	***N***	---	D,n	N,d	N,n	D,d
T20P8S1	***N***	***D***	***D***	***N***	***D***	***D***	***D***	***N***	---	D,d	D,n	D,d
T20P8S2	***N***	***D***	***D***	***N***	***D***	***N***	***D***	***D***	***D***	---	N,d	D,d
T30P8S1	***N***	***D***	***D***	***N***	***D***	***N***	***D***	***D***	***D***	***N***	---	D,d
T30P8S2	***N***	***D***	***N***	***D***	***N***	***N***	***D***	***D***	***D***	***D***	***D***	---

[1] T10 = temperature of 10 °C; T20 = temperature of 20 °C; T30 = temperature of 30 °C; P6 = pH of 6; P8 = pH of 8; S1 = tap water without added rock salt; S2 = tap water with rock salt concentration of 5000 mg/L; [2] D,d = significantly different; N,n = not significantly different (alpha = 0.05).

4. Discussion

Although the effect of increased hydraulic shear stress on streambank erosion is well established, relatively little is known about the effects of water chemistry (temperature, pH, and salinity) on cohesive streambank erosion. The small size and high specific surface area of clay minerals ensure that electrochemical forces such as attractions and linkages between clay sheets, rather than soil physical properties, primarily control their erosion behavior. While some previous studies have shown that water temperature, salinity, and pH can individually influence cohesive soil erosion [9], few experiments have directly studied the combination of these factors for different soil types. Results of this study clearly indicate that erosion rates increase with increasing stream water temperature for the two tested soils. Additionally, decreases in stream pH increase erosion rates, although the significance of this effect is a function of the ionic strength of the stream water and the amount of pH-dependent charge present in the dominant clay minerals.

To understand these results, it is important to note that the erosive behavior of cohesive soils is largely influenced by the amount and type of clay minerals they contain; therefore, an understanding of clay mineralogy and chemistry is important. The four most common clay minerals include kaolinite, smectite, illite, and vermiculite [9,12]; these four clays each exhibit differences in porosity, cation exchange capacity (CEC), expansion, plasticity, water adsorption, erodibility, and point of zero charge due to disparities in their physicochemical properties. Montmorillonite (a smectite) is a 2:1 clay with relatively low interlayer bonding strength, which gives it a large capacity to absorb water between the clay layers. Vermiculite is also a 2:1 clay but has a greater layer charge than montmorillonite, giving it a higher CEC but a lower capacity to expand in the presence of water. Therefore, montmorillonite is considered a fully expanding clay while vermiculite is considered as semi-expanding [40,41]. The charges associated with the surface of clay minerals are either permanent or variable. Permanent charges in clay minerals are a result of isomorphic substitutions, in which a cation substitutes another of similar size but different valence, leading to a net positive or negative charge. However, in most clay minerals, surfaces are negatively charged [42]. On the other hand, variable charges are charges at the surface of clay minerals that vary with pH due to the deprotonation or protonation of associated functional groups, especially the hydroxyl functional group, and the specific adsorption of cations and anions [43]. As a result, it is not surprising that the behavior of cohesive streambank soils is related to water chemistry.

Grissinger [44] studied the effects of the type and fraction of clay minerals, bulk density, moisture content at compaction, and clay mineral orientation on the erosion of mixtures of Grenada silt loam (base material) and industrial kaolin, montmorillonite, vermiculite, and illite clay minerals. However, during preliminary testing, increased flow temperature resulted in an increase in the rate of erosion, necessitating the control of water temperature during testing. Similarly, Zreik et al. [29] attributed increased erosion of the top 0.5 mm of cohesive sediment beds with increased flow temperatures to a reduction in clay bond strength with temperature. Changes in soil erosion rates with temperature could be attributed to changes in water density and viscosity, which result in increased hydraulic shear stress on the soil. For example, Raudkivi and Hutchinson [27] tested the effect of salinity and temperature on the surface erosion of fine and coarse-grained commercial kaolinites. Their results show that erosion rates first decreased with increasing temperature before they increased. The decrease in erosion rate with increased temperature was attributed to lowered flow viscosity resulting in lowered hydraulic shear, while the increase in erosion rate was attributed to increased 'intensity of molecular bombardment' at the surface of the clay minerals by eroding flow molecules, leading to a higher propensity for the detachment of surface particles. However, the explanation of changes in flow temperature leading to a lowered erosion rate via the mechanism of reduced hydraulic shear is unlikely as, within the range of testing temperatures, a 10 °C decrease in flow temperature (a greater temperature range than tested in Raudkivi and Hutchinson's study) results in a relatively insignificant decrease (about 5%) in hydraulic shear.

A more likely explanation for increases in erosion rate with increased water temperature is that increases in flow temperature provide additional thermal energy to the interlayer molecules, increasing the spacing between clay sheets, which then reduces soil resistance to detachment by flowing water. Kelly and Gularte [26] explained changes in the soil critical shear stress (minimum hydraulic shear stress required for soil erosion) with flow temperature and salinity using the rate process theory, in which the activation energy required for clay detachment is dependent on temperature. The authors attributed increases in erosion with increased temperature or energy. Kemper et al. [45] investigated the influence of clay content, organic matter content, and temperature on cohesion development in reconstructed natural cohesive soil and suggested that an increased rate of cohesion development at higher soil temperatures was partly a result of increased ionic solubility at a higher temperature. This may explain why, in our study, minor changes in Er/u* with temperature were generally observed at the higher salt concentration. Kelly and Gularte [26] also noted an inverse relationship between erosion and salinity. The observed increase in soil critical shear stress with salinity was attributed to an increased number of interparticle bonds per area with salinity, leading to an overall increase in the activation energy required for surface erosion.

Ravisanger et al. [46] studied the effect of sediment pH on the resuspension of kaolinite samples placed in a flume bed. The erosive behavior of the kaolin samples with pH was explained in terms of possible clay particle associations: face to face (FF), edge to face (EF), and edge to edge (EE). FF is van der Waals attraction between parallel clay minerals, EF is the electrostatic interaction between negatively charged faces and positively charged edges, and EE is the van der Waals attraction between clay edges. Study results show that the relationship between erosion rate and pH was in the form of an inverted V-shape: below pH 5.5, erosion rate decreased with decreasing pH due to the predominance of EF particle associations. As the pH increased to between 5.5 and 7, the structure of clay particles changed from EF to EE, resulting in increased erosion rates due to the relatively weaker bond structure of the van der Waals forces. Above pH 7, the authors hypothesized that the particles regrouped to form FF associations that, due to the increased surface contact, led to higher bond strengths and lower erosion rates.

Results of our study show that changes in erosion rate vary as a function of both salinity and pH and as a function of clay mineralogy. Based on the foregoing, the following is supposed: As pH increases, pH dependent or variable charge is altered due to deprotonation of surface functional groups; changes in surface charge may increase the number of possible bonds between the clay sheets and relative soil stability; at high sodium chloride concentrations, higher valence interlayer cations are likely displaced by relatively larger sodium ions, resulting in clay expansion and susceptibility to erosion. However, because the available sites for ionic exchange on the surface of a cohesive soil is influenced by pH (variable charge effects), the influence of salinity on erosion rate may be enhanced or negated by changes in pH, depending on the type of soil.

5. Conclusions

Results of this study clearly show that soil clay type and stream chemistry play a significant role in the fluvial erosion of cohesive streambanks. However, current stormwater regulations in the U.S. focus primarily on the control of peak flow rates (the highest stream flow during a storm event) to minimize downstream flooding and to prevent channel erosion. Based on the results of this study, stormwater management regulations should also consider controlling stream temperature to ensure channel stability as recent research has shown that water temperatures in urban areas can increase by over 8 °C during storm events [47,48]. While deicing salts are a concern for the biological integrity of streams [49], the effects of high levels of salinity on the stability of cohesive streambanks are more complex, as they depend on the dominant clay mineral and associated interlayer cations, as well as the stream pH and chemical composition of the road salt. Therefore, it is important to better understand the influence of stream chemistry on the erosion of cohesive streambanks to ensure stormwater management regulations protect channel stability.

Supplementary Materials: The following are available online at www.mdpi.com/xxx/s1, Table S1. Erosion rates, shear stresses, and zeta potential for each erosion experiment for a montmorillonite dominated and a vermiculite dominated soil.

Acknowledgments: Funding for this research was provided by the Virginia Tech Institute for Critical Technology and Applied Sciences (ICTAS).

Author Contributions: T.W.-T., W.G., and M.J.E. conceived and designed the experiments; W.G. and S.H. performed the experiments; S.H. and A.I.A. analyzed the data; S.H., A.I.A., W.G., T.W.-T., and M.J.E. wrote the paper.

Conflicts of Interest: The authors declare no conflict of interest. The founding sponsor had no role in the design of the study; in the collection, analyses, or interpretation of data; in the writing of the manuscript, and in the decision to publish the results.

References

1. ASCE Task Committee on Hydraulics; Bank Mechanics; Modelling of River Width Adjustment. River width adjustment. I: Processes and mechanisms. *J. Hydraul. Eng.* **1998**, *124*, 881–902. [CrossRef]
2. Pimentel, D.; Harvey, C.; Resosudarmo, P.; Sinclair, K.; Kurz, D.; McNair, M.; Crist, S.; Shpritz, L.; Fitton, L.; Saffouri, R.; et al. Environmental and economic costs of soil erosion and conservation benefits. *Science* **1995**, *267*, 1117–1123. [CrossRef] [PubMed]
3. Lawler, D.M. The impact of scale on the processes of channel-side sediment supply: A conceptual model. In *Effects of Scale on Interpretation and Management of Sediment and Water Quality, Proceedings of the Boulder Symposium, Boulder, CO, USA, 2–14 July 1995*; International Association of Hydrological Sciences Publication: London, UK, 1995; Volume 226, pp. 175–184.
4. Simon, A.; Curini, A.; Darby, S.E.; Langendoen, E.J. Bank and near-bank processes in an incised channel. *Geomorphology* **2000**, *35*, 193–217. [CrossRef]
5. Wynn, T.; Mostaghimi, S. The effects of vegetation and soil type on streambank erosion, southwestern Virginia, USA. *JAWRA* **2006**, *42*, 69–82. [CrossRef]
6. Osterkamp, W.R.; Heilman, P.; Gray, J.R. An Invitation to Participate in a North American Sediment-Monitoring Network. *Eos Trans. Am. Geophys. Union* **2004**, *85*, 40. [CrossRef]
7. Pizzuto, J.I.; The ASCE Task Committee on Hydraulics; Bank Mechanics; Modeling of River Width Adjustment. Streambank erosion and river width adjustment. In *Sedimentation Engineering*; Garcia, M.H., Ed.; American Society of Civil Engineers: Reston, VA, USA, 2007; pp. 387–438. ISBN 0784408149.
8. Moody, J.A.; Smith, J.D.; Ragan, B.W. Critical shear stress for erosion of cohesive soils subjected to temperatures typical of wildfires. *J. Geophys. Res. Earth Surf.* **2005**, *110*, F01004. [CrossRef]
9. Grabowski, R.C.; Droppo, I.G.; Wharton, G. Erodibility of cohesive sediment: The importance of sediment properties. *Earth Sci. Rev.* **2011**, *105*, 101–120. [CrossRef]
10. Heede, B.H. Designing for dynamic equilibrium in streams. *JAWRA* **1986**, *22*, 351–357. [CrossRef]
11. Schumm, S.A. *The Fluvial System*; Wiley: New York, NY, USA, 1977.
12. Zhu, Y.H.; Lu, J.Y.; Liao, H.Z.; Wang, J.S.; Fan, B.L.; Yao, S.M. Research on cohesive sediment erosion by flow: An overview. *Sci. China Ser. E Technol. Sci.* **2008**, *51*, 2001–2012. [CrossRef]
13. Lal, R.; Shukla, M.K. *Principles of Soil Physics*; Marcel Dekker, Inc.: New York, NY, USA, 2004; p. 716. ISBN 0824753240.
14. Sparks, D.L. *Environmental Soil Chemistry*; Elsevier: New York, NY, USA, 2003.
15. Winterwerp, J.C.; van Kesteren, W.M. *Introduction to the Physics of Cohesive Sediment in the Marine Environment*; Developments in Sedimentology; Elsevier: Amsterdam, The Netherlands, 2004; Volume 56, pp. 29–50.
16. Mitchell, J.K.; Soga, K. *Fundamentals of Soil Behavior*, 3rd ed.; Wiley: London, UK, 2005; pp. 143–169.
17. Santamarina, J.C. Soil behavior at the microscale: Particle forces. In Proceedings of the Symposium on Soil Behavior and Soft Ground Construction, Cambridge, MA, USA, 5–6 October 2001; MIT: Cambridge, MA, USA, 2001.
18. Carey, W.P.; Simon, A. *Physical Basis and Potential Estimation Techniques for Soil Erosion Parameters in the Precipitation-Runoff Modeling System (PRMS)*; U.S. Geological Survey Water-Resources Investigations Report 82-4218; U.S. Geological Survey: Nashville, TN, USA, 1984.

19. Zelazny, L.W.; He, L.; Vanwormhoudt, A.M. Charge analyses of soils and anion exchange. In *Methods of Soil Analysis: Part 3 Chemical Methods*; Sparks, D.L., Ed.; Soil Science Society of America: Madison, WI, USA, 1996; pp. 1231–1254.
20. Raudkivi, A.J. *Loose Boundary Hydraulics*, 4th ed.; A. A. Balkema: Rotterdam, The Netherlands, 1998; ISBN 9054104473.
21. Schoer, J.; Duwe, K. Sampling design for estuarine investigations. *TrAC Trends Anal. Chem.* **1986**, *5*, 128–131. [CrossRef]
22. Nelson, K.C.; Palmer, M.A. Stream temperature surges under urbanization and climate change: Data, models, and responses. *J. Am. Water Resour. Assoc.* **2007**, *43*, 440–452. [CrossRef]
23. Corsi, S.R.; Graczyk, D.J.; Geis, S.W.; Booth, N.L.; Richards, K.D. A fresh look at road salt: Aquatic toxicity and water-quality impacts on local, regional, and national scales. *Environ. Sci. Technol.* **2010**, *44*, 7376–7382. [CrossRef] [PubMed]
24. Mohseni, O.; Erickson, T.R.; Stefan, H.G. Sensitivity of stream temperatures in the United States to air temperatures projected under a global warming scenario. *Water Resour. Res.* **1999**, *35*, 3723–3733. [CrossRef]
25. Partheniades, E. *Cohesive Sediments in Open Channels*; Butterworth-Heinemann: Burlington, MA, USA, 2009; ISBN 1856175561.
26. Kelly, W.E.; Gularte, R.C. Erosion resistance of cohesive soils. *J. Hydraul. Div.* **1981**, *107*, 1211–1223.
27. Raudkivi, A.J.; Hutchison, D.L. Erosion of Kaolinite Clay by flowing water. *Proc. R. Soc. Lond.* **1974**, *337*, 537–544. [CrossRef]
28. Taylor, B.D.; Vanoni, V.A. Temperature effects in low transport, flat bed flows. *J. Hydraul. Div.* **1972**, *98*, 1427–1445.
29. Zreik, D.A.; Krishnappan, B.G.; Germaine, J.T.; Madsen, O.S.; Ladd, C.C. Erosional and mechanical strengths of deposited cohesive sediments. *J. Hydraul. Eng.* **1998**, *124*, 1076–1085. [CrossRef]
30. Harris, W.G.; Iyengar, S.S.; Zelazny, L.W.; Parker, J.C.; Lietzke, D.A.; Edmonds, W.J. Mineralogy of a chronosequence formed in New River alluvium. *Soil Sci. Soc. Am. J.* **1980**, *44*, 862–868.
31. Wynn, T.M.; Henderson, M.B.; Vaughan, D.H. Changes in streambank erodibility and critical shear stress due to subaerial processes along a headwater stream, southwestern Virginia, USA. *Geomorphology* **2008**, *97*, 260–273. [CrossRef]
32. Parks, O.W. Effect of Water Temperature on Cohesive Soil Erosion. Master's Thesis, Virginia Tech, Blacksburg, VA, USA, 12 December 2012.
33. Webb, P.A.; Orr, C. *Analytical Methods in Fine Particle Technology*; Micromeritics Instrument Corp.: Norcross, GA, USA, 1997; ISBN 096567830X.
34. Van Olphen, H. *An Introduction to Clay Colloid Chemistry*, 2nd ed.; John Wiley & Sons: New York, NY, USA, 1977; ISBN 047101463X.
35. Scales, P.J.; Grieser, F.; Healey, T.W. Electrokinetics of the muscovite mica-aqueous solution interface. *Langmuir* **1990**, *6*, 582–589. [CrossRef]
36. Kundu, P.K. *Fluid Mechanics*; Academic Press: San Diego, CA, USA, 1990; ISBN 0124120512.
37. Shapiro, S.S.; Wilk, M.B. An Analysis of Variance Test for Normality (Complete Samples). *Biometrika* **1965**, *52*, 591–611. [CrossRef]
38. Box, G.E.P.; Cox, D.R. An analysis of transformations. *J. R. Stat. Soc.* **1964**, *26*, 211–252.
39. Anderson, T.W.; Darling, D.A. Asymptotic theory of certain goodness-of-fit criteria based on stochastic processes. *Ann. Math. Stat.* **1952**, *23*, 193–212. [CrossRef]
40. Brady, N.C.; Weil, R.R. *The Nature and Properties of Soils*, 14th ed.; Pearson/Prentice Hall: Upper Saddle River, NJ, USA, 2008; ISBN 9332519102.
41. McBride, M.B. *Environmental Chemistry of Soils*; Oxford University Press: New York, NY, USA, 1994; ISBN 0195070119.
42. Barton, C.D.; Karathanasis, A.D. Clay minerals. In *Encyclopedia of Soil Science*, 3rd ed.; Lal, R., Ed.; CRC Press: Boca Raton, FL, USA, 2016; pp. 421–425. ISBN 1498738907.
43. Goldberg, S.; Lebron, I.; Seaman, J.C.; Suarez, D.L. Soil Colloidal Behavior. In *Handbook of Soil Sciences Properties and Processes*, 2nd ed.; Huang, P.M., Li, Y., Sumner, M.E., Eds.; CRC Press: Boca Raton, FL, USA, 2011; ISBN 1439803056.
44. Grissinger, E.H. Resistance of selected clay systems to erosion by water. *Water Resour. Res.* **1966**, *2*, 131–138. [CrossRef]

45. Kemper, W.D.; Rosenau, R.C.; Dexter, A.R. Cohesion development in disrupted soils as affected by clay and organic matter content and temperature. *Soil Sci. Soc. Am. J.* **1987**, *51*, 860–867. [CrossRef]
46. Ravisangar, V.; Dennett, K.E.; Sturm, T.W.; Amirtharajah, A. Effect of sediment pH on resuspension of kaolinite sediments. *J. Environ. Eng.* **2001**, *127*, 531–538. [CrossRef]
47. Somers, K.A.; Bernhardt, E.S.; Grace, J.B.; Hassett, B.A.; Sudduth, E.B.; Wang, S.; Urban, D.L. Streams in the urban heat island: Spatial and temporal variability in temperature. *Freshw. Sci.* **2013**, *32*, 309–326. [CrossRef]
48. Hester, E.T.; Bauman, K.S. Stream and retention pond thermal response to heated summer runoff from urban impervious surfaces. *J. Am. Water Resour. Assoc.* **2013**, *49*, 328–342. [CrossRef]
49. Kaushal, S.; Groffman, P.M.; Likens, G.E.; Belt, K.T.; Stack, W.P.; Kelly, V.R.; Band, L.E.; Fisher, G.T. Increased salinization of fresh water in the northeastern United States. *Proc. Natl. Acad. Sci. USA* **2005**, *102*, 13517–13520. [CrossRef] [PubMed]